Proceedings of the 20th International Conference on Soil Mechanics and Geotechnical Engineering– Rahman and Jaksa (Eds)

Separation of the primary and secondary consolidation of freeze-dried clay

Séparation de la consolidation primaire et secondaire de l'argile lyophilisée

Hideki Ohta
Research and Development Initiative, Chuo University, Japan, e-mail: ohta@tamacc.chuo-u.ac.jp

Tadayoshi Kondo, Tamotsu Hashimoto, Toshihiko Sakagami
Kawasaki Geological Engineering, Japan

Atsushi Iizuka
Research Center for Urban Security and Safety, Dept. of Civil Engineering, Kobe University, Japan

ABSTRACT: To determine the feasibility of observing primary and secondary consolidation separately in an oedometer test, a freeze-drying technique was adopted to develop a half-dried clay specimen. This technique, which removes the major part of pore water from the macropores of the specimen without the effect of capillary force, allows the double-layered water on the surface of clay particles to remain. Two approximately identical specimens of Holocene clay were subjected to oedometer tests, one immediately after being sampled from the ground, and the other after being half-dried. The creep settlement of the half-dried specimen was observed throughout the entire testing period because there was practically no pore water in the macropores, and hence the primary consolidation took place instantaneously after loading. As expected, these two oedometer tests showed that the creep settlements of the two specimens were almost identical when the settlement was plotted against the logarithm of elapsed time. However, unexpectedly, no immediate (elastic) settlement of the half-dried specimen was observed even at the very early stage of the testing period whereas the subsequent settlement linearly increased with the logarithm of time.

RÉSUMÉ : Afin de déterminer la faisabilité d'observer séparément la consolidation primaire et secondaire dans un test d'oedomètre, une technique de lyophilisation a été adoptée pour mettre au point un spécimen d'argile à moitié séché. Cette technique, qui élimine la majeure partie de l'eau des macropores de l'échantillon sans l'effet de la force capillaire, permet de maintenir la double couche d'eau à la surface des particules d'argile. Deux spécimens approximativement identiques d'argile holocène ont été soumis à des tests d'oedomètre, l'un immédiatement après avoir été prélevé dans le sol, et l'autre après avoir été à moitié séché. Le tassement par fluage de l'échantillon à moitié séché a été observé tout au long de la période d'essai car il n'y avait pratiquement pas d'eau interstitielle dans les macropores, et donc la consolidation primaire a eu lieu instantanément après le chargement. Comme prévu, ces deux tests sur oedomètre ont montré que les tassements par fluage des deux spécimens étaient presque identiques lorsque le tassement était tracé par rapport au logarithme du temps écoulé. Cependant, de manière inattendue, aucun tassement immédiat (élastique) du spécimen à moitié séché n'a été observé, même au tout début de la période d'essai, alors que le tassement ultérieur augmentait linéairement avec le logarithme du temps.

KEYWORDS: oedometer test, primary consolidation, secondary consolidation, creep settlement, freeze-drying technique

1 INTRODUCTION

Considering the unique relationship between compressive strain and effective stress, Terzaghi (1948) demonstrated that a one-dimensional consolidation of clays (later called primary consolidation) can be successfully defined by a differential equation of heat conduction type. Buisman (1936) conducted a long-term consolidation test for 500 d and demonstrated that the settlement due to secondary consolidation was proportional to the logarithm of elapsed time after loading. He mentioned that the 'secondary time effect' observed at a site was reported in America. He also introduced two cases of secondary settlement that increases linearly with the logarithm of time: i) long-term settlement of a road embankment reported by Royer, and ii) the observation of a dike settlement for two years. Since then, the creep settlement of clays has been recognized as an important secondary factor in estimating settlement–time curves. Figure 1 presents a summary of Bjerrum's work (1972), where he interpreted the diagenetic phenomenon of geo-materials during sedimentation processes relative to the creep settlement and provided physical meaning to the pseudo-over-consolidation effect of aged clays.

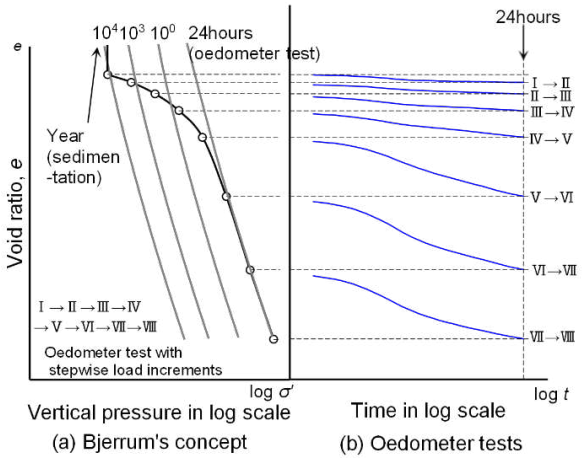

Figure 1. Bjerrum's concept of delayed compression.

In the oedometer tests on clay specimens with thicknesses of 20 mm, secondary consolidation is observed after primary consolidation, which is usually completed within 1 h. Until the end of the oedometer tests, the creep settlement observed during the secondary consolidation linearly increases with the logarithm of elapsed time after loading. This is a well-established experimental fact. However, embedded in the primary

consolidation, the secondary consolidation before the completion of the primary consolidation is not observable, as shown in Figure 2.

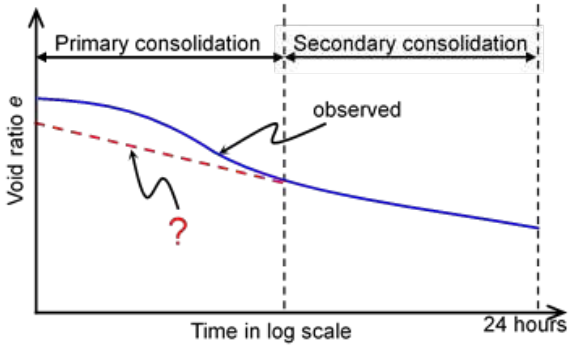

Figure 2. Creep in primary consolidation.

In the field, for example on embankment projects situated on soft clayey foundations, primary consolidation takes a significant number of years because the maximum drainage length is typically in the order of several meters. Secondary consolidation (creep settlement), which simultaneously develops during the period of primary consolidation, is also not observable in the field. To observe the secondary consolidation (creep settlement) which may start developing immediately after loading, it is necessary to complete the primary consolidation immediately after loading. This is achieved by removing major part of pore water from the macropores (Figure 3) without actually altering the micro-structures of the clay 'skeleton'.

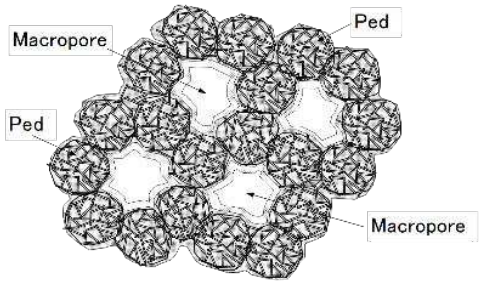

Figure 3. Ped and macropore.

In this paper, the term 'primary consolidation' is used vaguely, although it should be used in describing the consolidation process in which a unique relationship between the void ratio and effective stress is obeyed by the soil, whereas the term 'secondary consolidation' is one in which this condition is not satisfied. (Definitions given by Hawley, 1973.)

The pore water in clay specimens can be removed by air drying. However, this is accompanied by shrinkage of the clays owing to capillary force. Therefore, the developed specimens are not suitable for oedometer tests.

In this study, we introduced the freeze-drying technique to allow the observation of creep settlement owing to secondary consolidation throughout the entire testing period. In the oedometer test adopted in this investigation, a half-dried specimen was produced by removing the major part of the pore water from the macropores of the specimen without the effect of capillary force, thus, allowing the double-layered water to remain stationary on the clay particle surfaces. The creep settlement during the entire oedometer test process is described in this paper.

2 SPECIMEN PREPARATION AND TEST PROCEDURE

Two specimens of Holocene silty clay (with specific gravity of soil particle Gs = 2.690, liquid limit w_L= 59.70%, plastic limit w_P = 30.50%) were cut out of an undisturbed sample collected from a depth range of 14.0–14.8m at Kita-Katsushika near the mouth of the Ara River flowing into Tokyo Bay in Japan (Figure 4). One of the two specimens, N-(N: natural specimen, natural water content w_n = 57.21%, void ratio e = 1.539, pre-consolidation pressure p_c=167.8 kPa), was subjected to an oedometer test in the conventional way. The other specimen, D-(D: half-dried specimen, natural water content w_n = 57.54%, void ratio e = 1.548, pre-consolidation pressure p_c = 154.0 kPa), was half dried (water content w = 37.27%) by freeze - drying and then subjected to an oedometer test.

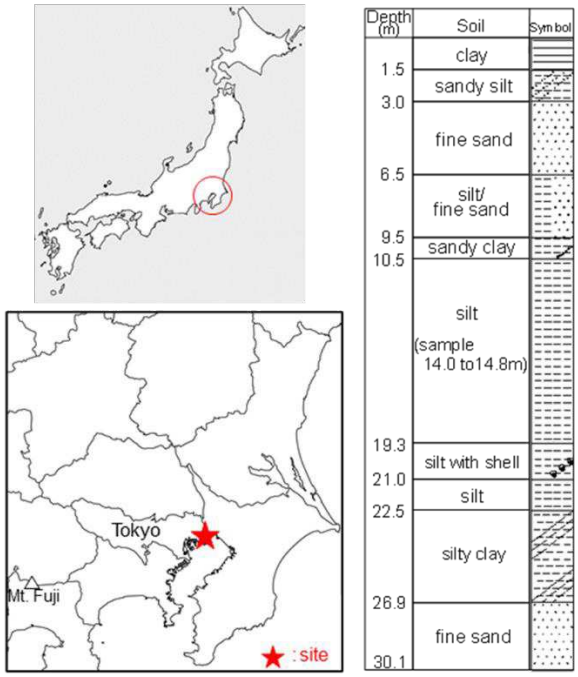

Figure 4. Site and boring log.

The water content of Specimen D decreased from w_n = 57.54% to w = plastic limit (w_P = 30.50%) + α% via the freeze-drying technique. In the preliminary tests, α was chosen at approximately 7%. The sublimation of the pore water in the frozen specimen subjected to vacuum pressure in a desiccator was accelerated by a cold trap (Figure 5) in which the vaporized pore water was frozen again. The weight of Specimen D in the process of drying in a desiccator was measured at a certain time interval until the water content reached the target.

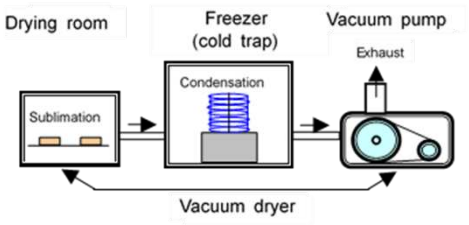

Figure 5. Cold trap.

In this study, it was demonstrated that the effect of light on the possible disturbance of the clay skeleton micro-structure (caused by freezing the water inside the pores), as well as on the possible loss of the double-layered water covering the clay particles (caused by the excessive removal of water) was negligible. To

reduce the friction difference between the side wall of the oedometer and Specimens N and D, the sides of the specimens were covered with a thin (0.006 mm thick) vinyl sheet wrapping the sidewall of the specimens, as shown in Figure 6. Preliminary tests indicate that this lubrication is effective in equalizing the side friction of testing specimens N and D.

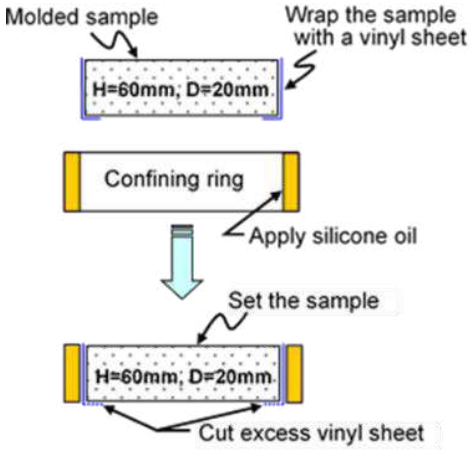

Figure 6. Friction reduction.

3 SEPARATION OF PRIMARY AND SECONDARY CONSOLIDATION

Figure 7, similar to Figure 1 (b), summarizes the results of the oedometer tests on Specimens N and D. Increase in the compressive strain, ε (ε = (e_0-e)/(1+e_0)) is plotted against log t, where the data points of triangles (▲) and circles (O) represent Specimens N and D, respectively.

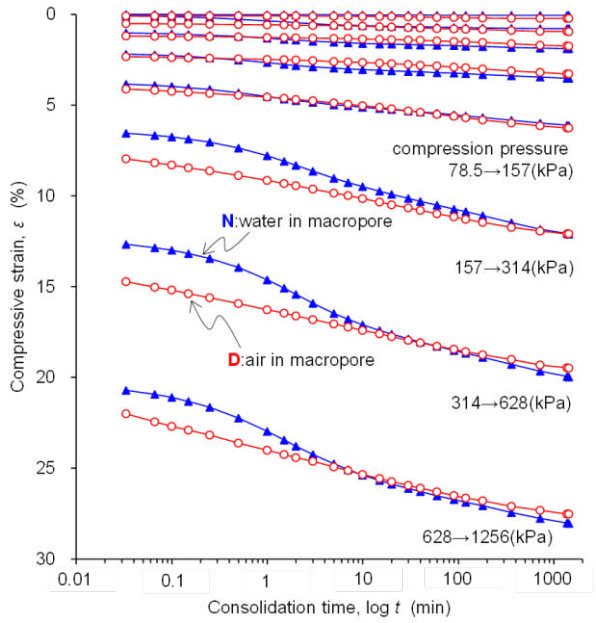

Figure 7. Compressive strain ε plotted against the logarithm of elapsed time t (ε–log t relationships).

In the first five loading steps (0 →9.8, 9.8 →19.6, 19.6 →39.2, 39.2 →78.5, and 78.5 →157.0 kPa), the specimens remained in the over-consolidated state, and primary consolidation was completed almost instantaneously. Hence, the data points of triangles ▲ (N) and circles O (D) overlapped. In the subsequent three loading steps (157→314, 314→628, and 628→1256 kPa), in which the specimens are already in the normally consolidated states, the increase in compressive strain ε of Specimen N (triangles ▲) is inhibited compared with that of Specimen D (circles O). This slow process of primary consolidation of Specimen N is, as is well known, caused by the slow speed of pore water flowing from macropores towards the outside.

The primary consolidation of Specimen N in normally consolidated states takes 20 to 30 min to be practically completed, as illustrated in Figure 7, while the secondary consolidation (creep) continues to occur until the end of each loading step (1440 min after loading). The secondary compression curves of Specimen N in normally consolidated states approximately overlap with those of Specimen D, which are nearly linear when plotted against the logarithm of elapsed time t. The major part of the volume of macropores in Specimen D is occupied by air that can be instantaneously expelled from macropores when the specimen decreases its volume owing to compression, that is, the primary consolidation of Specimen D takes place immediately after each loading. Data points represented by circles (O) indicate that the secondary consolidation starts before the primary consolidation is completed, giving an answer to the question in Figure 2.

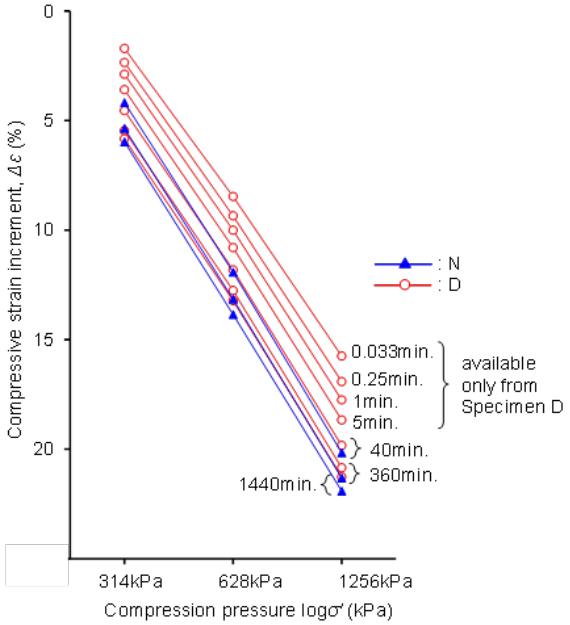

Figure 8. Compressive strain increment Δε plotted against the logarithm of compression pressure σ'.

(Compressive strain increment Δε is the difference between the current strain ε and the compressive strain at the end of the loading step from 78.5 kPa to 157 kPa.)

Figure 8 shows the two groups of the compressive strain increment Δε plotted against the logarithm of applied compression pressure σ'. One is a set of data obtained from the early stages of the oedometer test on Specimen D (circles O) shown in the upper half of the graph and the other consists of three couples of the data obtained from the oedometer tests on Specimens N (triangles ▲) and D (circles O) shown in the lower half of the graph. The compressive strain increment Δε is the difference between the current strain ε and the compressive strain at the end of the loading step from 78.5 to 157 kPa. The three couples of compressive strain increments Δε of Specimens N (triangles ▲) and D (circles O) shown in the lower half of the graph increase with the elapsed time during each loading step of

the compression pressures of 314, 628, and 1256 kPa (higher than pre-consolidation pressure) maintained for 1 day (1440 min). The two upper lines (one represented by triangles (▲) and the other by circles(O)) illustrate the data obtained at 40 min after each loading. The lowest and middle two lines are at 1440 min and 360 min, respectively. These two lines in each couple almost overlap, thus demonstrating that the creep behaviours of Specimens N and D are identical. Figure 8 is developed by examining the concept suggested by Bjerrum (1972), as shown in Figure 1 (a). It is evident that the test data proposed in this study agree optimally with Bjerrum's concept.

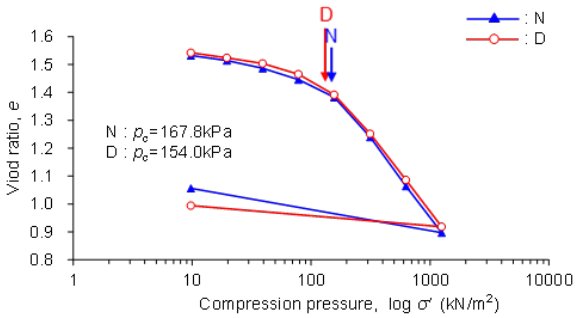

Figure 9. *e* – log σ' plots of oedometer tests on specimens N and D

In summary, the *e* – log σ' plots of the oedometer tests on Specimens N and D are shown in Figure 9 in a conventional manner. Figures 7, 8, and 9 demonstrate that the micro-structure of the frozen Specimen D is almost mechanically identical to that of Specimen N, which was not frozen.

4 CHANGE IN VOID RATIO IMMEDIATELY AFTER LOADING

To estimate the magnitude of instantaneous change in the void ratio of Specimen D immediately after applying each load increment, the test data such as shown in Figures 1 (a) and (b) are replotted in Figures 10.

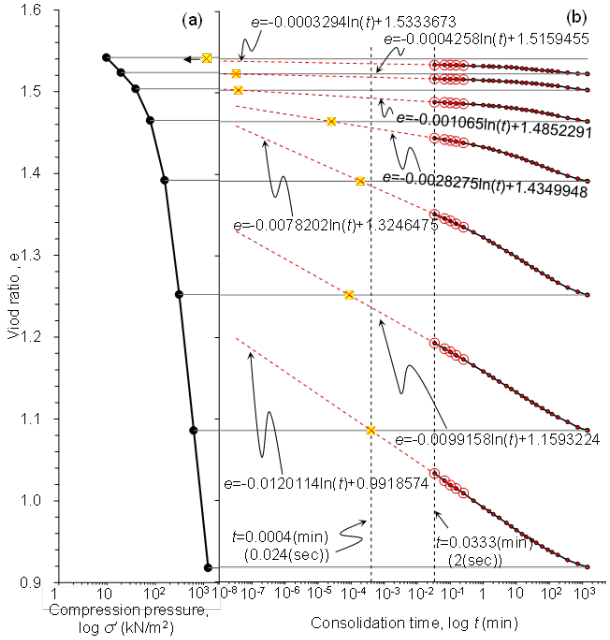

Figure 10. Extrapolation of data from oedometer test on Specimen D. (a) e – log σ' plots. (b) Extrapolation of *e* – log *t* curves.

In the oedometer test of Specimen D, although the current engineering practice in Japan requires the first reading to be made 6 s after the application of load, the first reading of the settlement was made 2 s after the application of each load increment. It has been conventionally accepted that the *e* – log *t* plots in the secondary consolidation stage are approximately represented by a single line. However, after examining the data summarized in Figure 10 (b), the authors concluded that it is appropriate for each of the 7 groups of the *e* – log *t* plots in Figure 10 (b) to be represented by 3 lines (beginning part starting at 2 s after loading, middle part, and final part that lasts until 1440 min) rather than one single line representing the data points from the beginning to the end of each loading period.

The eight solid circles in Figure 10 (a) represent the void ratio values of Specimen D at the beginning and end of each loading period. Horizontal lines starting from the solid circles in Figure 10 (a) and bridging in Figures 10 (a) and (b) indicate the void ratio values of Specimen D at the moment of applying new load increments except the horizontal line, which is located in the lowest part of Figure 10 because no additional load increment is applied further. The dotted lines in Figure 10 (b) represent the first 5 data points of the 7 groups of the e – log t plots. These 7 dotted lines represent the beginning part of the 7 groups of data points. Seven cross symbols (×) in Figure 10 (b) are specified as the crossing points of the seven dotted lines and seven horizontal lines starting from seven data points in Figure 10 (a). These 7 symbols (×) indicate the elapsed time after load application when the compressive deformation starts increasing from zero. This estimate is acceptable only when the extrapolation of the dotted lines is justifiable. However, such justification is left for future work because the authors have no verifiable back data yet. As observed in Figure 10 (b), these 7 symbols (×) exhibit time shorter than 0.0004 min (0.024 s), i.e., 8.73×10^{-12} min (5.24×10^{-10} s), 3.27×10^{-8} min (1.96×10^{-6} s), 3.84×10^{-8} min (2.31×10^{-6} s), 2.51×10^{-5} min (1.51×10^{-3} s), 1.89×10^{-4} min (1.13×10^{-2} s), 8.65×10^{-5} min (5.19×10^{-3} s) and 3.99×10^{-4} min (2.40×10^{-2} s) from top to bottom.

This means that Specimen D did not experience any 'instantaneous deformation', and all subsequent deformations were creep deformations, which increased linearly with the logarithm of elapsed time. Immediately after the application of the load increment at each loading stage, Specimen D does not experience any instantaneous (elastic) compressive deformation, but only the time dependent (creep) deformation. This may be valid under conditions where the extrapolation, represented by the dotted lines, is applicable, as illustrated in Figure 10 (b). When the authors planned the oedometer tests on Specimens N and D several years ago, this unexpected finding was beyond the scope of the authors who initially intended to only observe the creep settlement of clay specimens during a period in which the primary consolidation was in progress.

5 DEFINITION OF PRIMARY CONSOLIDATION

Curve ① in Figure 11 shows that the expected creep strain increases with the time elapsed after loading in the oedometer test on Specimen D. Curve ② represents the strain instantaneously induced by the application of load and remains unchanged as long as the load is kept constant. Curve ③ is the summation of the instantaneous (elastic) strain Curve ② and the creep (time-dependent) strain of Curve ①. Curve ① was traditionally expected to be inferior in its magnitude of strain compared to Curve ②. When planning the oedometer test on Specimen D, the authors expected to experimentally obtain a curve to indicate the possible relationship between compressive strain and elapsed time after applying a constant consolidation

pressure, as illustrated by Curve ③ in Figure 11.

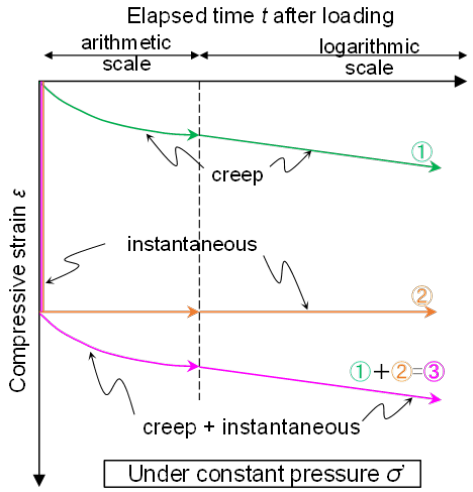

Figure 11. Expected strain-time relations.

However, the experimentally obtained actual strain–time relationships are similar to Curve ①, as shown in Figures 10. No instantaneous part of the strain was observed during the period in which extrapolation is applied, as shown in Figure 10 (b). Because it is unclear at the present stage whether creep strain of consolidated clays increases linearly with the logarithm of elapsed time, even in a very short period of time after loading, further discussion will be made assuming that there is an absence of instantaneous strain, as tentatively concluded in Section 4.

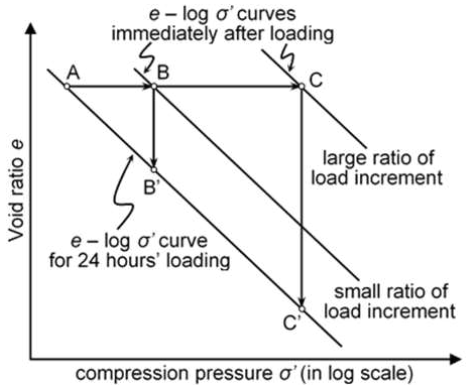

Figure 12. Schematic diagram showing the location of the e – log σ' relationships for zero-loading time (immediately after loading).

When we extend Bjerrum's concept described by combing Figures 1 (a) and 8, a schematic diagram presented in Figure 12 is obtained, thus indicating the feature of the e – log σ' relationships experienced by a soil element located at the drainage boundary (where the excess pore water pressure dissipates immediately after the application of a load increment) in oedometer tests. In Figure 12, the state of a specimen at the end of a loading stage is represented by point A on the line of the e – log σ' relationship for a 24 h loading period. When an additional load increment is applied, point A moves to point B or C depending on the load increment ratio (=additional load/load before the application of additional load). Then, points B and C move to B' and C', respectively. Points B' and C' may not be on the same line because the e – log σ' relationship for the 24 h loading period may also be slightly influenced by the load increment ratio. This was in agreement with the study carried out by Leonards (1962), which showed the void ratio e plotted against the logarithm of effective stress σ' (e – log σ' curve) obtained from a test with a higher load increment ratio located at a lower position (smaller e) than that with a lower load increment ratio. It can be observed that the e – log σ' relationships for the zero-loading time (immediately after loading) strongly depend on the load increment ratio. The lines for equal-loading time are located between the line of zero-loading time and that of the 24 h loading time, as experimentally shown in Figure 8. It should be noted that the location of the e – log σ' relationships for the zero-loading time (immediately after loading) depends not only on the load increment ratio, but also on the load sustaining time of the previous loading step.

The classical theories of one-dimensional consolidation are conventionally built on five basic assumptions, as summarized in Figures 13 (a) and (b), Terzaghi (1948), and Mikasa (1963). For the nonlinear relationship between effective stress and void ratio, Davis and Raymond (1965) derived equations that look similar to Terzaghi's equation. McNabb (1960) derived the equation in the same form as Mikasa's equation.

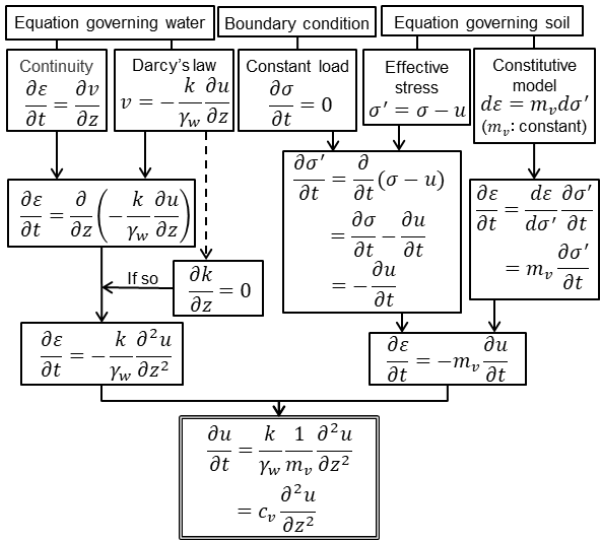

(a) Terzaghi's basic equation of consolidation

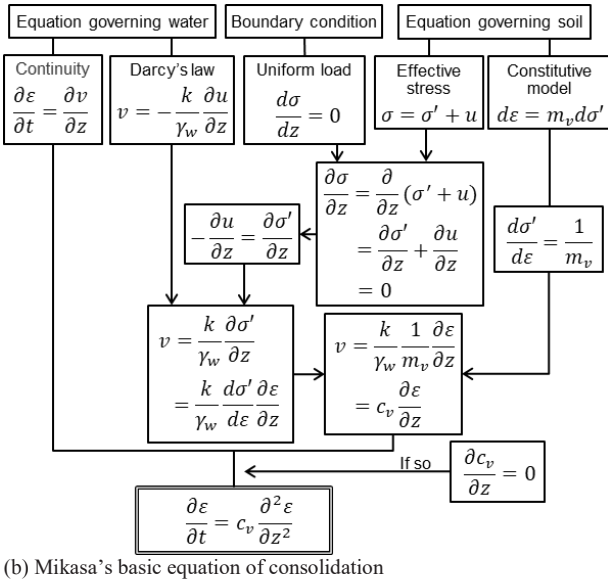

(b) Mikasa's basic equation of consolidation

Figure 13. Derivation of basic equations of consolidation proposed by Terzaghi and Mikasa.

Both Terzaghi's and Mikasa's basic differential equations of one-dimensional consolidation were developed starting from the following five basic assumptions:

(1) continuity, (2) Darcy's law, (3) definition of effective stress,

(4) constitutive model and (5) boundary condition.

As summarized in Figures 13 (a) and (b):

1. The decrease in the volume of clay is equal to the amount of pore water flowing out (equation of continuity in which v and z are mean velocities of flowing water and depth),
2. The velocity v of water flowing through soils is governed by Darcy's law, in which k represents permeability,
3. Effective stress σ' is defined as the total stress σ minus the pore water pressure u,
4. Strain increment dε is proportional to effective stress increment dσ', and
5. The constant load is represented by $\partial\sigma/\partial t = 0$ in Terzaghi's derivation and the uniform load by $\partial\sigma/\partial z = 0$ in Mikasa's derivation.

The equations of Terzaghi and Mikasa are similar in their form except for the variables: excess pore pressure u in Terzaghi's equation and compressive strain ε in Mikasa's equation. As observed in Figures 13 (a) and (b), only the difference in deriving Terzaghi's and Mikasa's basic equations is present in the boundary condition, constant load in Terzaghi's, and uniform load in Mikasa's. Both differential equations proposed by Terzaghi and Mikasa are in the form of a heat conduction type. The experimental findings mentioned in Section 4 indicate that m_v in the constitutive model assumed by Terzaghi and Mikasa is zero or close to zero: thus, the constitutive model assumed in the 1-D consolidation theories of Terzaghi and Mikasa loses its physical meaning. This means that the mathematical derivation processes shown in Figures 13 (a) and (b) may not be justifiable. In conventional consolidation theories, the non-time-dependent strain increment is indispensable as a function of the effective stress increment. This requirement needs to be critically reviewed. Based on the possible conclusion drawn from the experimental works, in which there was practically no or negligible (so called) elastic compressive strain in the primary consolidation process, material parameter m_v in constitutive models required in theories of primary consolidation must be a function of both, the effective stress and the elapsed time after loading. The logical consequence of this study would possibly be that little or no primary consolidation process conceptually described by classical consolidation theories can be justified. We may need novel interpretations to explain the phenomenon we refer to as 'primary consolidation'.

Hawley (1973) defined the primary and secondary consolidation processes as follows: 'A primary consolidation process is one in which a unique relationship between voids ratio and effective stress is obeyed by the soil. A secondary process is one in which this condition is not satisfied'. The constitutive model in Figures 13 (a) and (b) is a unique relationship between the effective stress and compressive strain $\varepsilon = (e_0\text{-}e)/(1+ e_0)$, which is not time dependent. However, definition of "primary consolidation" is a new problem arising from the discussion above.

6 CONCLUSIONS

To effectively observe secondary consolidation (creep settlement) that may start immediately after loading, it is necessary to bring the primary consolidation to completion instantaneously after loading. This was achieved by removing a major part of the pore water from the macropores in clays (i.e., by producing a half-dried clay specimen) via a freeze-drying technique. From the results of the oedometer test on half-dried clay, it was inferred that instantaneous (elastic) compressive deformation experienced by the half-dried clay immediately after the application of load increment at each loading stage was negligible, and only the subsequent deformation was time dependent (creep). Because this result was unexpected, it should be verified by carrying out more testing in the future.

The following conclusions were derived:

(1) The e – log σ' relationships for the zero-loading time (immediately after loading) are dependent not only on the load increment ratio, but also on the load sustaining time of the previous loading step.

(2) Material parameters in constitutive models required in theories of primary consolidation must depend not only on effective stress but also on elapsed time after loading. Hawley and Borin (1973) proposed a consolidation theory that takes the time effect ($^{de}/_{dt}$ where e denotes the void ratio and t denotes time) into the relationship between the effective stress σ' and void ratio e.

(3) Novel interpretations may be required to explain the phenomena we refer to as 'primary consolidation' and 'secondary consolidation'. Akai et al. (1984) conducted a long-term (50 d) triaxial Ko-consolidation test in which the coefficient of earth pressure at rest, Ko, continuously increased during the entire process of secondary consolidation to Ko=0.77 after 50 d from Ko = 0.52 at the start, which was observed when the primary consolidation was almost complete. Although their test was completed on the 50th day, the test data indicated that Ko would become even higher if the test was carried out longer. The mechanism of secondary consolidation may be closely related to the continuous change in the effective stress state. Consolidation is, in fact, a two-dimensional process rather than purely one-dimensional.

7 ACKNOWLEDGEMENTS

The authors are grateful for the invaluable assistance of Mr. T. Hamada and Mr. S. Yamabe of Kawasaki Geological Engineering in preparing the manuscript, to Dr. Y. Morikawa of the National Institute of Maritime, Port and Aviation Technology for helpful suggestions, and to Prof. M. J. Pender of the University of Auckland for his comments on the paper during its preparation. The authors would like to thank Editage for the English language editing.

8 REFERENCES

Akai K., Sano I., Ma S. D. and Ishiguro T. 1984. Experimental studies on delayed consolidation, Disaster Prevention Research Institute Annual Report, Kyoto University, No 27, B-2, 49-63.

Bjerrum L. 1972. Embankments on soft ground, Proc. Specialty Session on 'Performance of earth and earth-supported structures', ASCE, Vol. II, 1-54.

Buisman A.S.K. 1936. Results of long duration settlement tests, Proc. 1st Int. Conf. Soil Mech. & Foundation Engrg, F-7, 103-106.

Davis E.H. and Raymond G.P. 1965. A non-linear theory of consolidation, *Geotechnique* 15, 161-173.

Hawley J.G. and Borin D.L. 1973. A unified theory for consolidation of clays, Part 1 Use of the term 'primary' and 'secondary' by J.G. Hawley and Part 2 The unified theory by J.G. Hawley and Borin, D.L. Proc. 8th Int. Conf. Soil Mech & Foundation Engrg, Moscow, Vol. 1.3, 2/18, 107-119.

Leonards G.A. 1962. Engineering properties of soils, Foundation Engineering edited by Leonards, G. A., McGraw Hill. 66-240.

McNabb A. 1960. A mathematical treatment of one-dimensional soil consolidation, *Quartery of Applied Mathematics*, Vol. 17, No.4, 337-347.

Mikasa M. 1963. *Consolidation of soft clays*, Kajima Shuppankai, in Japanese.

Terzaghi K. 1948. *Theoretical Soil Mechanics*, John Wiley, New York. 271.